Journal of Petroleum Exploration and Production Technology (2023) 13:1575–1589
https://doi.org/10.1007/s13202-023-01624-3

ORIGINAL PAPER-PRODUCTION ENGINEERING

Superstructure optimization of subsea processing layouts

Leonardo Sales[1] · **Milan Stanko**[1] · **Johannes Jäschke**[2]

Received: 22 August 2022 / Accepted: 7 March 2023 / Published online: 17 April 2023

Abstract

As the oil and gas industry expands the use of subsea processing, the complexity of subsea layouts increases, making manual design processes cumbersome and suboptimal. Here we propose a method to support subsea field design where optimization is performed on a model of the subsea system, to maximize the net present value of the project. The proposed mixed-integer nonlinear (MINLP) model is solved to compute a global optimum design considering constraints in production, equipment duties and cost, and reliability and maintenance aspects. The subsea layout, equipment capacity, oil and gas production rates, and system pressures are optimized. The method was applied on a synthetic field based on the Goliat field in the Barents Sea. The method successfully finds the best designs, while the second and third-best layouts give general insights for subsea processing layout optimization.

Keywords Field architecture · Decision-support tool · Concept selection · Offshore production systems

Sets

i	Set of superstructure flows $\{i_1, i_2, ...i_{17}\}$
j	Set of equipment $\{j_1, j_2, ..j_{12}\}$
m	Set of flowlines and risers $\{fg, rg, fm, rm, fo, ro\}$
t	Time-step [years] $\{t_1, t_2, ...t_{10}\}$

Variables

α	Overall operating time [h/year]
Δp	Pressure difference in the compressor [kPa]
$\mathbf{b}(t)$	RHS for mass balance for time step t [ton/h]
$\mathbf{x}(i,t)$	Mass flow i for time step t [ton/h]
$\mathbf{y}$	Binary variables for subsea unit installation [–]
A_c	Installed heat transfer area [m^2]
C_0	Initial investments [million USD]
$c_1(p_{\text{in}})$	Multiphase pump duty coefficient [kJ/(kg kPa^2)]
$c_2(p_{\text{in}})$	Multiphase pump duty coefficient [kJ/(kg kPa)]
C_{c}	Cooler cost [million USD]
C_{k}	Compressor cost [million USD]
C_p	Pump cost [million USD]
C_{fg}	Gas flowline cost [million USD]
C_{fm}	Multiphase flowline cost [million USD]
C_{fo}	Oil flowline cost [million USD]
C_{mpp}	Multiphase pump cost [million USD]
C_{rg}	Gas riser cost [million USD]
C_{rm}	Multiphase riser cost [million USD]
C_{ro}	Oil riser cost [million USD]
C_{ss}	Subsea separator cost [million USD]
C_{ts}	Topside separator cost [million USD]
CF(t)	Cash flow for time step t [million USD]
f_{r}	Reliability factor [–]
G(t)	Gas production rate for time step t [ton/h]
NPV	Net present value [million USD]
O(t)	Oil production rate for time step t [ton/h]
$\text{P}_{\text{k}}(t)$	Compressor duty for time step t [kW]
p_{s}	Pressure at the inlet of the separation station [kPa]
p_{in}	Boosting equipment inlet pressure [kPa]
$P_{\text{k,max}}$	Maximum compressor power consumption [kW]
$P_{\text{mpp}}(t)$	Multiphase pump duty for time step t [kW]
p_{out}	Boosting equipment outlet pressure [kPa]
$P_{\text{p,max}}$	Maximum pump power consumption [kW]
$P_{\text{p}}(t)$	Pump duty for time step t [kW]
$p_{\text{r}(t)}$	Reservoir pressure for time step t [kPa]
$q_{\text{ppo}}(p_{\text{s}})$	Maximum initial production potential for separator pressure p_s [ton/h]
$q_{\text{pp}}(t)$	Maximum production potential for time step t [ton/h]
$\text{R}_{\text{f}}(t)$	Recovery factor [%wt]
$x_{\text{c,max}}$	Cooler maximum installed capacity [ton/h]
$x_{\text{p,max}}$	Pump maximum installed capacity [ton/h]

✉ Leonardo Sales
leonardopasaleseng@gmail.com

[1] Department of Geoscience and Petroleum, NTNU, S.P. Andersens veg 15, 7031 Trondheim, Norway

[2] Department of Chemical Engineering, NTNU, Sem Sælands vei 6, 7034 Trondheim, Norway

$x_{ss,max}$ Subsea separator maximum installed capacity [ton/h]

$x_{ts,max}$ Topside separator maximum installed capacity [ton/h]

Introduction

Motivation

Subsea processing is a relatively new approach for recovering oil resources and may be a key enabler for many challenging field developments. It can be defined as the handling, treatment and production of produced fluids on the seabed. Typical examples include separation, compression and pumping processes. Subsea processing can be very advantageous for deeper waters, and to make marginal fields profitable, so its usage is expected to increase in the future. Here, we want to investigate the impacts of subsea processing in the layout optimization of subsea systems. To this end, a mixed-integer nonlinear (MINLP) model which contains subsea processing equipment options is solved to find the global optimum design of the field layout.

The oil and gas industry has the ambition to expand the use of subsea processing in existing and future fields, as seen around the world in the last years. Figure 1a shows the number of subsea processing units for several locations around the world. Most of the deployments are concentrated in Norway, UK, Brazil and USA. Figure 1b shows the number of planned and existing subsea processing units in time depicting water depth, while Fig. 1c shows the existing and planned subsea processing units in time depicting tieback distance. There is a significant increase in the use of subsea processing in the last two decades along with water depth and tie-back distance.

There are many advantages of using subsea processing. It increases safety (due to fewer personnel travelling and having contact with equipment), increased recovery, and ultimately economic value. The benefits also increase with flow-rates, water depth, and the exploitation of marginal fields (Albuquerque et al. 2013; John et al. 2018). It also can reduce the waste disposal to the sea, operational risks (as the processing equipment is on the seabed) and the environmental footprint, as smaller platforms, or none at all, are used.

Subsea processing may reduce capital expenditures (CAPEX), as it allows to connect satellite fields to existing infrastructure nearby, often extending their lifetime. Adding subsea processing may also postpone the need to upgrade the existing topside facilities to handle new operating conditions. This is especially important when upgrading topside facilities is not feasible due to space restrictions, and building another topside is the only option, thus

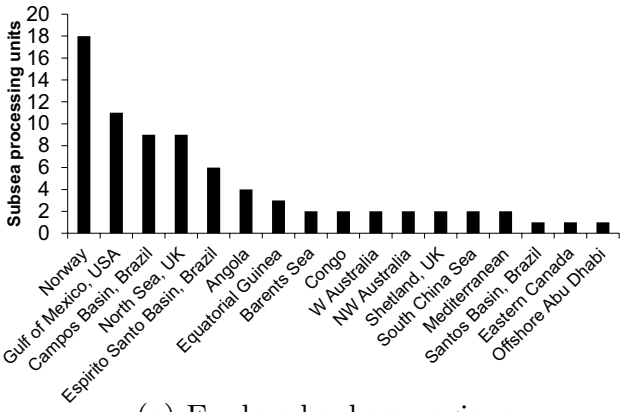

(a) Explored subsea regions

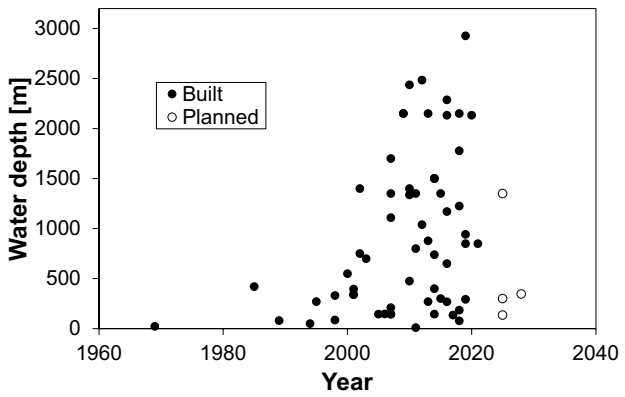

(b) Explored subsea water depth

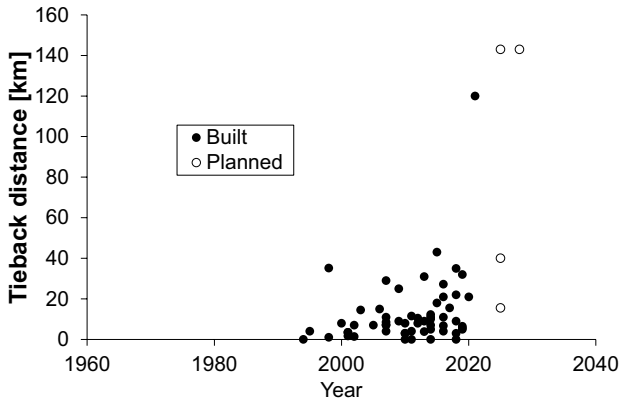

(c) Explored subsea tieback distance

Fig. 1 Current subsea trends. Data extracted from Offshore Magazine (2020)

dramatically reducing cost and the environmental impact related to manufacturing.

The use of subsea processing, however, creates new challenges that neither existed nor were required in earlier projects (Moreno-Trejo et al. 2012; Økland et al. 2013). Determining the optimal layout of the subsea processing system, type and number of equipment, operating conditions and capacity, is one of them. Several studies have previously

considered layout optimization of petroleum production systems, but mostly focused on topside or equipment location, without a specific focus on subsea processing systems and equipment allocation (Hong et al. 2017; Liu et al. 2022; Mnasri et al. 2022).

Previous work

In the following part, we will limit our review to studies dealing with methods based on numerical optimization and mathematical programming to provide decision support when designing and operating petroleum production systems.

Studies in this area started arranging the subsea equipment as a secondary objective, while the topside arrangement was prioritized. Devine and Lesso (1972) employed a general model to minimize oil field development costs, but the only subsea facilities considered were flow-lines. The first relevant work in optimization of subsea layout was published by Grimmett and Startzman (1987), where a binary programming approach was employed for sizing and placing topside and subsea facilities (i.e. platforms, templates and manifolds). As binary implicit enumeration was used, the method managed to find the absolute minimum investment development plan, but even the small-sized case study contained nearly 10^{190} development options, making it unfeasible for large applications. Later research (Garcia-Diaz et al. 1996) was conducted to overcome this and other problems.

Rosa and Ferreira Filho (2013), Rodrigues et al. (2016) and Sales et al. (2018) proposed methods of optimizing subsea layout by locating and allocating topsides and manifolds. Rosa and Ferreira Filho (2013) developed an exhaustive search model that maximizes NPV, while Rodrigues et al. (2016) proposed an integer linear programming model for the same problem. Sales et al. (2018) proposed a Monte Carlo simulation approach combined with a genetic algorithm to address uncertainties in the placement of topsides and manifolds. In these studies, no other subsea equipment was considered besides flow-lines and manifolds.

Recently published works focus on optimizing gathering systems (i.e. spatially optimizing networks of flow-lines, pipelines, and manifolds). Fonseca dos Santos et al. (2017) proposed an evolutionary algorithm to find the best position for the topside and subsea equipment, while considering marine geology, environmental constraints, offshore operations, risers anchoring, and others. Stape et al. (2019) analysed the selection of manifold and trunk line strategies and their impact on costs and production rates using a genetic algorithm. They also observed that uncertainties play a key role in the optimum layout. This and other recent studies (Chidiac et al. 2019; González et al. 2020; Angga and Stanko 2021; Sales et al. 2021; Bilal et al. 2021) focus on other aspects of field development without addressing subsea design.

Díaz Arias et al. (2021) avoids the use of a superstructure approach by combining evolutionary algorithms (EA) and commercial simulation software to automate and optimize concept selection and field architecture design when considering decentralized subsea processing modules. The algorithm solves the field layout design problem with a great deal of precision, but it does require high computational effort.

One major point lacking in previous studies is that the subsea design does not include the presence of subsea processing equipment. To overcome this, Krogstad (2018) and Díaz Arias et al. (2021) dealt with the optimization of subsea processing systems. Krogstad (2018) proposed an MINLP model using the concept of superstructures to maximize the NPV of the planning and development of offshore oil field structures, considering a wide range of subsea equipment. The approach managed to obtain optimum solutions, along with useful insights, in short time. The main objective of this research is to expand and continue this study.

Main contributions

In this work, we continue and expand the model presented by Krogstad (2018). An MINLP optimization model where we maximize the net present value (NPV) of the project by varying the layout, flow-rates, equipment capacity, and system pressure is proposed. The model is constrained by production potential equations, compressor, pump and multiphase pump duties, equipment cost, reliability and maintenance aspects, and discharge equations. While Krogstad (2018) successfully optimizes the subsea field layout, we propose some key improvements in this model. Our contributions are the following:

- To model the production deliverability of the system upstream the subsea station, we employ a deliverability equation that depends on the recovery factor and inlet pressure to the subsea station;
- We consider that the pressure at the outlet of the subsea station depends on the produced flow-rates of oil, gas and water;
- We estimate the duty of the multiphase booster with a more rigorous method using correlations derived from HYSYS instead of using dry gas equations;
- We include maintenance and reliability aspects by adding penalties to uptime and operational expenditures due to the presence of equipment.

In the next section, the optimization model is presented. After, we show and discuss the results of the case study, then we conclude about the model's performance and its

applicability, relevance and potential advantages for subsea layout optimization.

Methodology

Optimization model

General approach

We approach the problem of subsea processing optimization using a superstructure approach. Superstructures represent all solutions expected by the designer combined. This approach was initially used for process synthesis in chemical engineering plants (Umeda et al. 1972) and still is widely applied. Figure 2 illustrates the subsea layout superstructure used in the present study. The superstructure accounts for subsea separation (cooler and separator), boosting (compressor, multiphase and oil pump), and surface equipment (risers and topside separator). If multiphase flow is chosen, a separator must be installed at the FPSO. Else, the pressure of the phases must be increased separately by installing an oil pump and a gas compressor. A cooler is installed to condense out any remaining liquid before the compression. The condensed liquid is then commingled with the oil flow to the pump. All the fluids are produced to an FPSO.

We propose an MINLP model to find the combination of equipment that maximizes NPV. The decision variables are the selected equipment in the superstructure, the flow-rates, equipment capacity, and system pressure. The constraints are the reservoir deliverability, compressor, pump and multiphase pump duties, equipment cost, reliability and maintenance aspects, and discharge equations.

In the formulation, oil, gas and water rates are treated in units of mass over time, instead of standard volume over time. The main equations of the optimization model are shown below. More details are provided in Appendix A and Appendix C and in the work by Krogstad (2018). Due to nonlinearities in the equations and the binary variables regarding equipment presence, the problem is formulated as an MINLP.

All the flows are represented by continuous variables **x**. The subsea equipment (separator, compressor, pumps, and others) are represented by binary variables **y**. The optimal solution is represented by the set of optimal flow-rates, system pressure, equipment, and equipment capacity.

The mass balance in the nodes of the superstructure shown in Fig. 2 can be modelled by a set of linear equations represented by the equation below, that involves the matrix **A**, the flow-rates $\mathbf{x}(t)$, and the right-hand side of the balance, $\mathbf{b}(t)$

$$\mathbf{A}\mathbf{x}(t) = \mathbf{b}(t) \tag{1}$$

Economic optimization criteria

The objective function (Eq. 2) is set to maximize the NPV of the project, where C_0 is the initial investment, $CF(t)$ is the cash flow for the time step t, and r the interest rate.

$$\max \text{NPV} = -\frac{C_0}{1+r} + \sum_t \frac{\text{CF}(t)}{(1+r)^t} \text{ [million USD]} \tag{2}$$

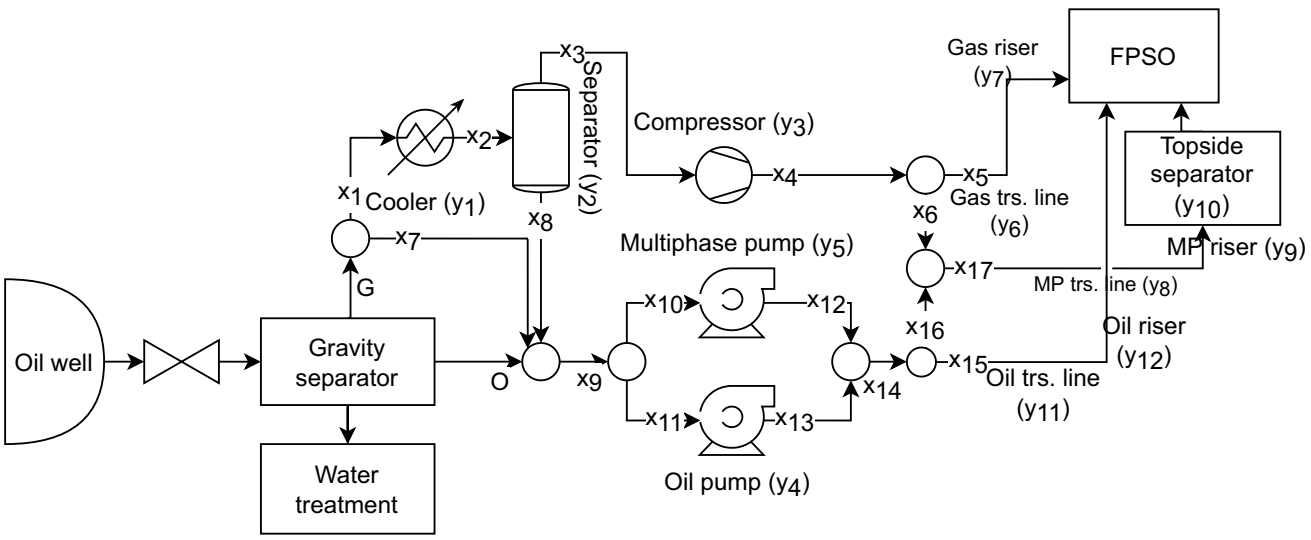

Fig. 2 Superstructure with subsea processing. The arrows point the flow direction between the units. The nodes represent mixing or splitting points

The cash flow CF(t) is defined as the difference between the revenue and operating costs (in million dollars)

$$\mathrm{CF}(t) = \left(\frac{\mathrm{O}(t)}{\rho_{\mathrm{o,std}}} p_{\mathrm{o}} + \frac{\mathrm{G}(t)}{\rho_{\mathrm{g,std}}} p_g\right)\alpha - \left(P_{\mathrm{k}}(t) + P_{\mathrm{p}}(t) + P_{\mathrm{mpp}}(t)\right) \cdot p_{\mathrm{e}} \cdot \alpha \tag{3}$$

where $\rho_{\mathrm{o,std}}$ and $\rho_{\mathrm{g,std}}$ are the oil and gas at standard-conditions, respectively. O(t) and G(t) are the oil and gas production rate for time step t calculated at the end of the year using a backward approximation, and p_{o}, p_{g}, and p_{e} are the oil, gas and electricity prices. We assume that the power is provided from shore or a neighbouring field; therefore, the energy consumption costs are considered in the model. $P_{\mathrm{k}}(t)$, $P_{\mathrm{p}}(t)$ and $P_{\mathrm{mpp}}(t)$ are, respectively, the compressor, oil pump, and multiphase pump duties. We do not consider other operational expenses.

The reliability factor f_r reduces the base operating hours per year (α_0) by some percent, simulating the increased chance of emergency stops in the production system according to the equipment j employed:

$$\alpha = \alpha_0 \cdot f_r \tag{4}$$

where

$$f_r = 1 - \sum_j r_{\mathrm{p}}(j) \cdot y(j) \tag{5}$$

while α is the overall operating hours per year, and $r_{\mathrm{p}}(j)$ is the reliability penalty assigned to each equipment, shown in the following vector. These values were chosen based on engineering insight, assuming that a failure in one equipment causes a loss of 1–5 days of the systems' annual reliability.

$$r_p(j) = \begin{bmatrix} 0.005 \\ 0.005 \\ 0.030 \\ 0.010 \\ 0.060 \\ 0.001 \\ 0.001 \\ 0.001 \\ 0.001 \\ 0.001 \\ 0.001 \\ 0.001 \end{bmatrix} \begin{matrix} \text{Cooler} \\ \text{Separator} \\ \text{Compressor} \\ \text{Oil pump} \\ \text{Multiphase pump} \\ \text{Gas flowline} \\ \text{Gas riser} \\ \text{Multiphase flowline} \\ \text{Multiphase riser} \\ \text{Topside separator} \\ \text{Oil flowline} \\ \text{Oil riser} \end{matrix} \tag{6}$$

The reliability penalty of each equipment, $r_{\mathrm{p}}(j)$ indicates that, if included, the equipment will cause a reduction in the expected total uptime of the system. For example, the presence of a compressor causes a yearly decrease in uptime of 3% due to maintenance work.

Simplified reservoir model equations

The maximum oil production (production potential) delivered by the system upstream the subsea processing station is a function of the recovery factor ($\mathrm{R_f}$) and the pressure at the suction of the subsea station (p_{s}):

$$q_{\mathrm{pp}}(t) = q_{\mathrm{ppo}}(p_{\mathrm{s}}) \cdot \left(a_1 \cdot \mathrm{R_f}(t)^3 + a_2 \cdot \mathrm{R_f}(t)^2 + a_3 \cdot \mathrm{R_f}(t) + 1\right) \text{ [ton/h]} \tag{7}$$

where a_1, a_2, a_3 are coefficients, and the recovery factor is the ratio of extracted oil over the oil initially in place (O_{IIP}):

$$\mathrm{R_f}(t) = \frac{\sum_{\tau=1}^{t} O(\tau)\,\alpha}{O_{\mathrm{IIP}}} \text{ [\%wt]} \tag{8}$$

The maximum initial production potential (q_{ppo}) is dependent on the pressure at the inlet of the separation station (p_s):

$$q_{\mathrm{ppo}}(p_{\mathrm{s}}) = q_{\mathrm{ppo,0}} \cdot \left[1 - b_1 \frac{p_{\mathrm{s}}}{p_{\mathrm{ref}}} - b_2 \left(\frac{p_{\mathrm{s}}}{p_{\mathrm{ref}}}\right)^2\right] \text{ [ton/h]} \tag{9}$$

where b_1 and b_2 are constants, p_{ref} is the reference pressure (which is equal to the static pressure when there is no flow at the inlet of the subsea station at the initial conditions) and $q_{\mathrm{ppo,0}}$ is the maximum initial production potential when $p_{\mathrm{s}} = 0$.

Equipment capacity

The compressor, oil pump and multiphase pump duties depend on the flow-rate through the unit and the pressure boost required. The compressor duty is given by Eq. 10, and the oil pump duty by Eq. 11.

$$P_k(t) = \frac{x_3(t)}{\eta_k} \cdot \frac{R \cdot T_i}{3.6 M_m} \cdot \frac{\gamma}{\gamma - 1}\left[\left(\frac{p_{\mathrm{out}}}{p_{\mathrm{in}}(t)}\right)^{\frac{\gamma-1}{\gamma}} - 1\right] \text{ [kW]} \tag{10}$$

where $x_3(t)$ is the compressor flow rate, η_k is the compressor efficiency, R the universal gas constant, T_i the gas temperature at the inlet of the compressor, M_m the natural gas molar mass, γ the heat capacity ratio of the gas, p_{in} the boosting equipment inlet pressure and p_{out} the boosting equipment outlet pressure. It is assumed that the compression is adiabatic.

The oil pump duty is given by

$$P_p(t) = x_{11}(t)\,\frac{p_{\mathrm{out}} - p_{\mathrm{in}}(t)}{3600 \rho_o \eta_p} \text{ [kW]} \tag{11}$$

where $x_{11}(t)$ is the pump flow rate and η_p is the pump efficiency. In this equation, we are assuming that the density of

oil at the pump inlet is similar to the density of the standard oil conditions.

To determine the duty of the multiphase pump, the total mass flow of the stream was multiplied by the isentropic enthalpy difference and divided the result by the isentropic efficiency. A constant isentropic efficiency of 60% was assumed. The following equation was used

$$P_{\text{mpp}}(t) = \frac{x_{10}(t) \cdot \Delta h_s}{\eta_{\text{mpp}}} \tag{12}$$

where $x_{10}(t)$ is the multiphase pump mass flow rate, η_{mpp} is the multiphase pump efficiency and Δh_s is the isentropic enthalpy difference.

The isentropic enthalpy difference was computed from a correlation derived using data from several simulations performed with HYSYS. The isentropic enthalpy difference is a function of the inlet pressure and the delta pressure across the pump. The inlet temperature is assumed fixed and equal to 70 °C. The composition employed for the simulation is provided in Table B.1 in Appendix B. The gas-oil ratio is assumed to be equal to 150 Sm^3/Sm^3 and constant in time. The adjusted curves have the form:

$$\Delta h_s = c_1\left(p_{\text{in}}\right) \cdot \Delta p^2 + c_2\left(p_{\text{in}}\right) \cdot \Delta p \tag{13}$$

where $\Delta p = p_{\text{out}} - p_{\text{in}}(t)$, and c_1 and c_2 are the coefficients given by

$$c_1\left(p_{\text{in}}\right) = -1.35\times10^{-7} - \frac{4.03\times10^{-6}}{1 + \left(\frac{p_{\text{in}}}{4299}\right)^{5.15}} \quad \left[\text{kJ}/\left(\text{kg kPa}^2\right)\right] \tag{14}$$

$$c_2\left(p_{\text{in}}\right) = 9.52\times10^{-3} + \frac{3.86\times10^{-2}}{1 + \left(\frac{p_{\text{in}}}{4468}\right)^{3.61}} \quad \left[\text{kJ}/(\text{kg kPa})\right] \tag{15}$$

We consider a choke element between the reservoir and the suction of the subsea station, therefore

$$p_r \geq p_{\text{in}}(t)\ [\text{kPa}] \tag{16}$$

and the pressure loss between the suction of the subsea station and the inlet of boosting equipment, as well as inside the subsea station, was considered negligible, therefore

$$p_s = p_{\text{in}}\ [\text{kPa}] \tag{17}$$

where $p_r(t)$ is the reservoir pressure. Equation 16 proved to be an algorithmic bound in our analyses. That is, although it is not active, adding this constraint speeds up the optimization.

More details about the formulation and the equations employed are given in Appendix A.

Solver strategy

The model was implemented in the high-level mathematical optimization system GAMS 37.1.0 (GAMS Development Corporation 2021) and solved with two different MINLP solvers, BARON 21.1.13 (Sahinidis 2021) and DICOPT (Kocis and Grossmann 1989), both with their default settings. These solvers were selected because they have the overall best performance for solving this problem.

DICOPT is an example of a commercial solver that uses outer approximation to discover local solutions to MINLP problems. In the outer approximation algorithm, an alternate sequence of MILPs and NLPs are solved. NLP problems are formed and solved by fixing the discrete variables, yielding an upper bound as the solution. The MINLP problem is then linearized around that solution, generating a MILP problem, which when solved yields the problem's lower bound as another solution. The discrete element of this solution is then fed into the NLP problem in order to update the upper bound. When the upper and lower bounds meet, the algorithm terminates.

Although methods like the outer approximation can perform efficiently and provide good solutions, they do not always find the global optimum. For many problems, the global optimum is difficult to recognize and even more difficult to locate, especially for MINLPs. To this type of problem, the spatial branch and bound algorithm is widely used (Liberti 2008). Convex envelopes are used to surround the non-convex functions to produce convex relaxations of the original problem. By solving the convex problem, a solution is obtained, which is used as the split point of the feasible space. The split regions are again surrounded by convex envelopes and the process is repeated until the optimal value of the subproblem is identified. If the lower bound of the first subregion is found to be higher than the upper bound of the second region, there is no need to continue searching for the global minimum in first subregion and so it can be discarded. The subregion who has the lowest value is then the region who has the global optimum solution. Several other algorithms have been derived from spatial branch and bound, including the branch and reduce algorithm used by the commercial solver BARON.

Both solvers ran on an Intel i9-990 processor and 32 GB RAM with a time limit of 48 h. The relative optimality gap for termination was set to 0.1% for BARON. The optimality gap shows the distance between the current best-found solution, and the overestimated upper bound of the problem, so it is safe to assume that the solution obtained by BARON is very close to, or at the global maximum of the problem.

The overestimated upper bound solution is unfeasible since it violates the mass balance, flow-rates, system pressure and equipment capacity variables equations, overall producing more oil than possible. However, it returns similar values regarding NPV.

BARON obtained the global optimum within reasonable computational time, however, only when the time span was small (i.e. 10 years). For a larger time span, the optimality gap was too large to conclude that the global optimal solution was obtained. The solution returned by DICOPT was slightly worse than the solution obtained by BARON. This happens because DICOPT does not guarantee global optimality. Therefore, BARON should be employed when obtaining the global optimum is important, while DICOPT may be used for simulation-optimization approaches that require fast results, such as Monte Carlo or control applications. Here, our approach will focus on using BARON.

Results

The case study presented here is based on the Goliat field, presented by Krogstad (2018). Relevant information about the field is given in Appendix C. The BARON solver converged in all cases with a relative optimality gap of 1×10^{-3}.

It is important to note that the problem does not contain only integer variables, but a nonlinear problem intrinsically connected to it. And, regarding the integer variables, there are few combinations possible for the case study. We enumerated all and obtained only 12. Solving the 12 nonlinear problems took about 3 s in the same computer. However, by increasing the number of variables (i.e. increasing number of equipment, time-steps, or equations), the number of feasible combinations increases exponentially, which drives the model to be computationally intractable. Therefore, the enumeration approach will most likely not be efficient for larger instances of this problem and it will be complex to implement. Even though it is a good idea to reduce the number of combinations to test by using other techniques, such as enumeration, the aim of this research was to make the model generic and require as little as possible practical "engineering" input. Solving the problem this way also reduces the chance of additional human errors, while providing a computational time still compatible with practical applications.

Table 1 Optimal set of binary variables for Structure A, B, and C

Description	Variable	Solution A	Solution B	Solution C
Cooler	y_1	1	1	0
Separator	y_2	1	1	1
Compressor	y_3	1	1	0
Oil pump	y_4	1	1	0
Multiphase pump	y_5	0	0	1
Gas transport line	y_6	0	1	0
Gas riser	y_7	0	1	0
Multiphase transport line	y_8	1	0	1
Multiphase riser	y_9	1	0	1
Topside separator	y_{10}	1	0	1
Oil transport line	y_{11}	0	1	0
Oil riser	y_{12}	0	1	0

Finding optimal and suboptimal layouts

Solving the model with BARON requires 8 s for a time span of 10 years and a time resolution of one year. Figure 3a shows the structure of the optimum solution found, Fig. 4 shows the optimum production curves, with an NPV of 1.72 billion USD, Fig. 5 shows the upper and lower bound trajectories versus computational time, and Table 1 shows the optimum binary variables of Structure A, B, and C. This structure employs subsea separation, boosting the gas phase through a compressor and the oil phase through an oil pump. The phases are later recombined and transported in a multiphase riser. This solution is similar to the one employed in the Åsgard field (Micali and Abelsson 2016).

In any field layout optimization problem, there may exist other layouts that are not part of the global optimum, but are relevant anyway. To further investigate sub-optimal field layout structures (such as the second or third best structures), we applied integer cuts in the model to exclude the global optimum. First, $\mathbf{y}$ was converted into a binary value, in the form $y_{\text{bin}} = \sum_j 2 \cdot y(j)^{j-1}$. Then, constraints were added to remove a specific y_{bin} from the search space, such as $y_{bin} \geq a$,

Table 2 NPV difference between structures

	NPV [million USD]	Compared to structure A	Revenue [million USD]	CAPEX [million USD]	OPEX [million USD]
Structure A	1720.9	0.00%	1740.4	18.01	2.28
Structure B	1718.8	−0.08%	1738.8	17.61	2.42
Structure C	1638.4	−4.75%	1661.9	18.46	5.1

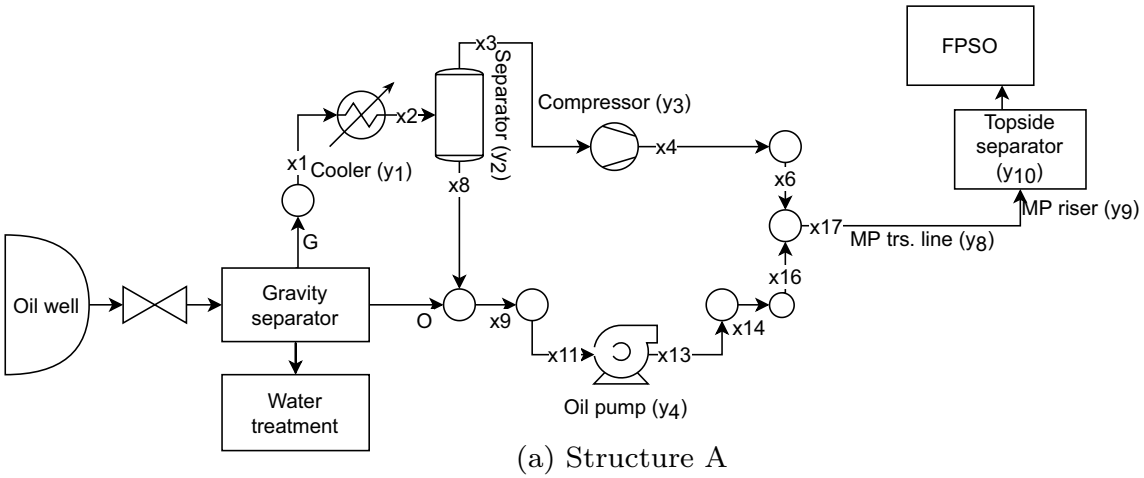

(a) Structure A

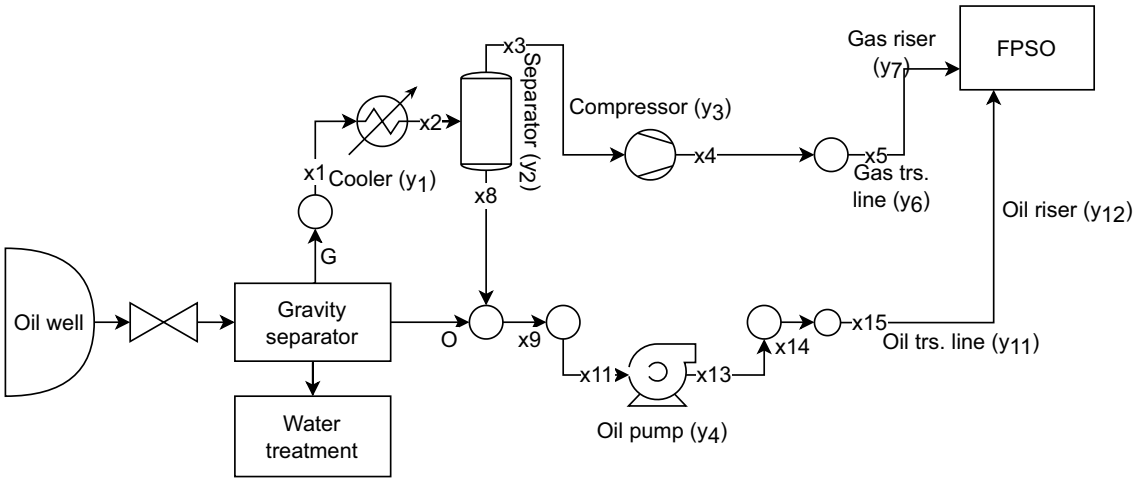

(b) Structure B

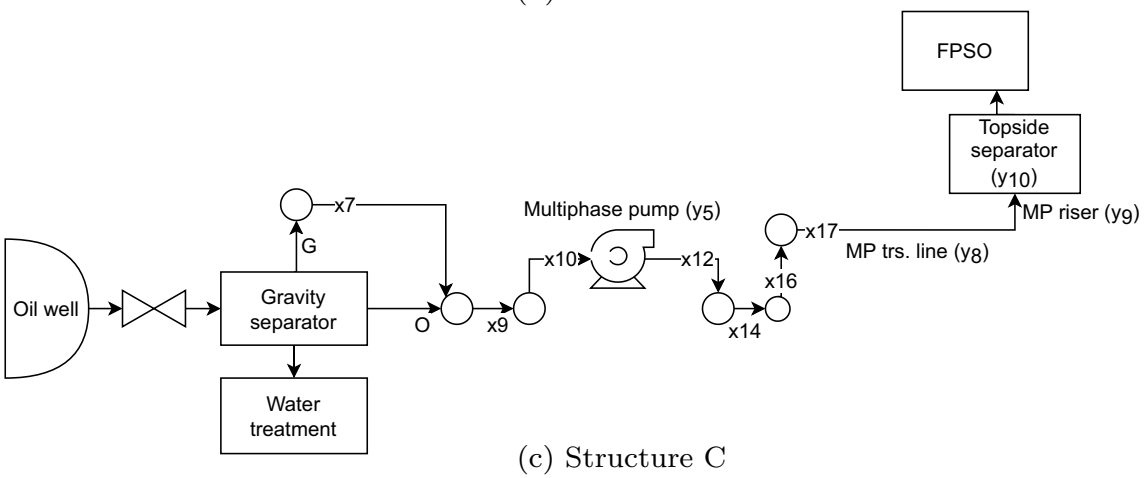

(c) Structure C

Fig. 3 First, second and third best structures obtained

and $y_{\text{bin}} \leq b$, where **a** and **b** are integer cuts. The values of **a** and **b** were selected by varying the range between a and b manually and evaluating if the solution changed. The whole range of feasible integer solutions was investigated. In this way, we removed the best layout design (Fig. 3a) from the feasible space, thus obtaining the second best layout, structure B (Fig. 3b). To obtain the third best layout, structure C

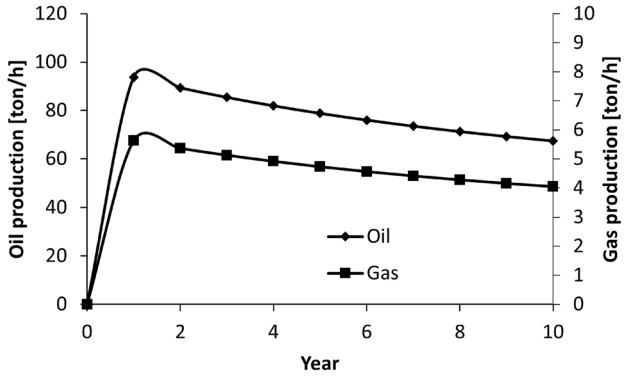

Fig. 4 Optimum production curves

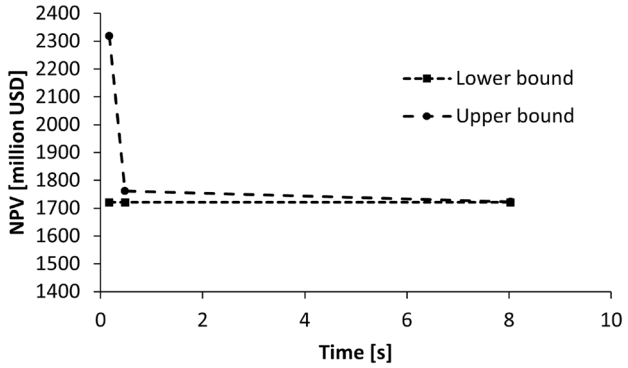

Fig. 5 Lower and upper bound curves versus computational time

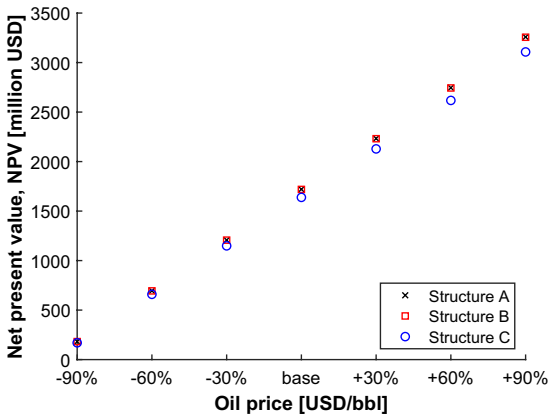

(a) Oil price

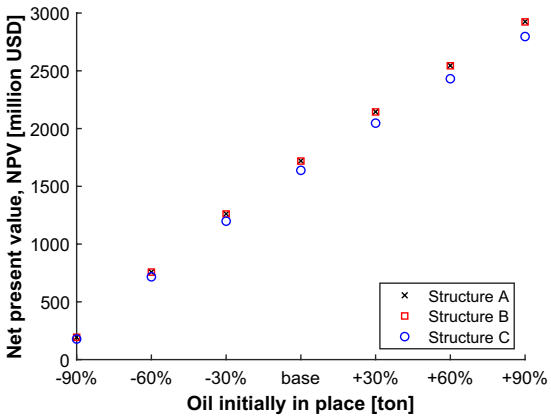

(b) Oil initially in place

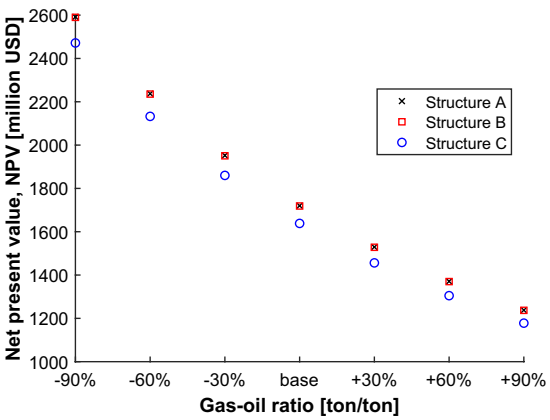

(c) Gas-oil ratio

Fig. 6 Sensitivity analyses for each parameter. The base is the original case, while the increase or decrease in the parameter is given by the percentage values

(Fig. 3c), we removed the first and the second best layouts from the feasible space.

Structure A employs full subsea processing and boosts the oil and gas in a single multiphase line. Structure B also employs full subsea processing, but it boosts the oil and gas in separate lines. These two layouts have a marginal difference in NPV (Table 2). Structure C ignores subsea separation completely and boosts oil and gas in a single multiphase line. The NPV difference between the first and third layout is small. The difference lies in revenue (due to lost revenue), operational and equipment costs, as seen in Table 2. Nonetheless, a preferred solution can be selected based on the user preferences and constraints.

The solution flow-rates, system pressure and equipment capacities were also analysed. They are the continuous variables of the problem and together with the structure, compose the solution of the field design problem. The best 5000 solutions were extracted from the solver. In all these solutions, the continuous variables had very similar values, thus obtaining a similar NPV. This is a challenge for the solver and it explains why it requires a high number of iterations to obtain the global optimum. This should be taken in mind while developing and implementing subsea layout optimization problems.

Sensitivity analysis over field parameters

We investigated the impact of some parameters on the NPV through a sensitivity analysis. We considered the following: oil initially in place (OIIP), oil price, and gas-oil ratio (GOR). The oil price had the biggest impact on the optimization results, followed by the OIIP and the GOR. Structures A and B are more robust than structure C for all studied scenarios.

For reduced values of oil price, oil initially in place, and gas-oil ratio, the three solutions are identical in terms of NPV. Figure 6 shows that for increasing values of OIIP and oil price, and decreasing values of GOR, structure C gets away from structures A and B in terms of NPV. This means that structure C is less robust for the given field. It seems that employing subsea processing is the best strategy for this case study, while the decision of boosting oil and gas in a single or a separate line is less relevant.

The reliability parameters also seem to have a large impact on the optimal solution. For example, if the reliability penalty factor for the multiphase pump is changed from 3 to 6%, structure C becomes optimal instead of structure A. Even though it is a small variation in the penalty factor, they play a key role in the subsea layout design, therefore it is important to properly estimate maintenance and reliability factors.

Discussion

A subsea layout optimization tool that considers subsea processing was developed. The tool successfully finds the best subsea processing design in the study case analysed. The model is based on Krogstad (2018), but significant changes and improvements were performed to make it more realistic, e.g. production deliverability, maintenance and reliability aspects, power consumption of multiphase boosters, and pressure calculations at the outlet of the subsea station.

In the convergence process of the model, NPV values close to the optimum are achieved in short time and with a few iterations, but a significant portion of the computation time is spent converging to the global optimum. A large part of the search space has similar values regarding NPV, flow-rates, system pressure, equipment capacity variables and equipment binaries. This fact could be exploited to find solutions faster, e.g. to run some initial optimization to find the equipment binaries and later to run another optimization with the equipment binaries fixed to converge on the continuous variables.

For the case studied, we note that structures A, B and C have a similar NPV. From a practical decision-making perspective, and given the precision of the estimations in our model, these solutions are equivalent. However, in the sensitivity analysis, we notice that structures A and B, which use subsea separation and boosting, are more robust to changes in oil price, OIIP and gas-oil ratio than structure C, which only uses subsea boosting.

Cost estimates for various subsea equipment, especially for multiphase pumps, have room for improvement. Maintenance cost estimation could be improved by collecting better data for several key parameters: downtime, mean time to failure and availability-independent maintenance costs. Other potential changes could include the ability to have different equipment in parallel, or the potential to have standby units available. Finally, the proposed methods were applied for a specific field only. More studies with other fields are required to guarantee the conclusions shown here.

We also suggest computing other key performance indicators to evaluate the difference between the solutions. Some key performance indicators that might be relevant to include are: internal rate of return, payback time and environmental performance factors such as CO_2 footprint, CO_2 emissions and energy consumption.

Finally, the value of the reliability penalty of the multiphase booster had a big impact on the optimal subsea processing layout. This shows that it is important to properly estimate maintenance and reliability factors.

Conclusions

1. The subsea layout optimization tool which considers subsea processing successfully finds the best subsea processing design in the study case analysed. The changes and improvements performed make the model more realistic.
2. The importance of improving maintenance and reliability aspects in the model is especially clear, as it obtained a more precise solution than the one seen in previous studies.
3. Nonetheless, by using an exact approach, a large amount of time is spent converging to the optimum.

Appendix A. Supplemental equations

The oil flow-rate is constrained by the maximum production potential

$$O(t) \leq q_{\text{pp}}(t) \text{ [ton/h]} \tag{18}$$

The gas flow-rate is given by

$$G(t) = \text{GOR}_{\text{mass}} \cdot O(t) \text{ [ton/h]} \tag{19}$$

where GOR_{mass} is the gas-oil ratio (in mass terms) and the reservoir pressure is assumed to decrease linearly from $p_{r,0}$ by a parameter β:

$$p_r(t) = p_{r,0} - \beta \cdot R_f(t) \text{ [kPa]} \tag{20}$$

The GOR can also be calculated in volume terms by $\text{GOR}_{\text{volume}} = \frac{V_{\text{g,std}}}{V_{\text{o,std}}}$, where $V_{\text{g,std}}$ is the volume of gas produced in standard conditions and $V_{o,std}$ the volume of oil produced in standard conditions. In mass terms, this ratio is simply the mass of gas produced divided by the mass of oil produced: $\text{GOR}_{\text{mass}} = \frac{m_{\text{g}}}{m_{\text{o}}}$.

The matrix $\mathbf{A}$ is based on the mass balances of the superstructure in Fig. 2. In order to avoid complex thermodynamic calculations in the model constraints, we assume that 5% of the gas stream is condensed in the cooler:

$$\mathbf{A} = \begin{bmatrix}
1 & 0 & 0 & 0 & 0 & 0 & 1 & 0 & 0 & 0 & 0 & 0 & 0 & 0 & 0 & 0 & 0 \\
1 & -1 & 0 & 0 & 0 & 0 & 0 & 0 & 0 & 0 & 0 & 0 & 0 & 0 & 0 & 0 & 0 \\
0 & 0.05 & 0 & 0 & 0 & 0 & 0 & -1 & 0 & 0 & 0 & 0 & 0 & 0 & 0 & 0 & 0 \\
0 & -1 & 1 & 0 & 0 & 0 & 0 & 1 & 0 & 0 & 0 & 0 & 0 & 0 & 0 & 0 & 0 \\
0 & 0 & -1 & 1 & 0 & 0 & 0 & 0 & 0 & 0 & 0 & 0 & 0 & 0 & 0 & 0 & 0 \\
0 & 0 & 0 & -1 & 1 & 1 & 0 & 0 & 0 & 0 & 0 & 0 & 0 & 0 & 0 & 0 & 0 \\
0 & 0 & 0 & 0 & 0 & 0 & 1 & 1 & -1 & 0 & 0 & 0 & 0 & 0 & 0 & 0 & 0 \\
0 & 0 & 0 & 0 & 0 & 0 & 0 & 0 & -1 & 1 & 1 & 0 & 0 & 0 & 0 & 0 & 0 \\
0 & 0 & 0 & 0 & 0 & 0 & 0 & 0 & 0 & -1 & 0 & 1 & 0 & 0 & 0 & 0 & 0 \\
0 & 0 & 0 & 0 & 0 & 0 & 0 & 0 & 0 & 0 & -1 & 0 & 1 & 0 & 0 & 0 & 0 \\
0 & 0 & 0 & 0 & 0 & 0 & 0 & 0 & 0 & 0 & 0 & 1 & 1 & -1 & 0 & 0 & 0 \\
0 & 0 & 0 & 0 & 0 & 0 & 0 & 0 & 0 & 0 & 0 & 0 & 0 & -1 & 1 & 1 & 0 \\
0 & 0 & 0 & 0 & 0 & 1 & 0 & 0 & 0 & 0 & 0 & 0 & 0 & 0 & 0 & 1 & -1
\end{bmatrix} \tag{21}$$

The vector $\mathbf{b}(t)$ is thus given by

$$\mathbf{b}(t) = \begin{bmatrix} G_t & 0 & 0 & 0 & 0 & 0 & -O_t & 0 & 0 & 0 & 0 & 0 & 0 & 0 & 0 \end{bmatrix}^T \text{ [ton/h]} \tag{22}$$

The following equations set the flow-rates of the unused units to zero (in ton/h):

$$x_1(t) \leq U\, y_1 \tag{23}$$

$$x_2(t) \leq U\, y_2 \tag{24}$$

$$x_7(t) \leq U\, y_5 \tag{25}$$

$$x_{10}(t) \leq U\, y_5 \tag{26}$$

$$x_{11}(t) \leq U\, y_4 \tag{27}$$

$$x_5(t) \leq U\, y_6 \tag{28}$$

$$x_6(t) \leq U\, y_8 \tag{29}$$

$$x_{15}(t) \leq U\, y_{11} \tag{30}$$

$$x_{16}(t) \leq U\, y_8 \tag{31}$$

The use of certain equipment may prevent the use of another. To consider this, logical constraints are employed. First, the system requires the installation of either the multiphase pump, or the combined installation of both the compressor and the oil pump

$$y_3 + y_5 - 1 = 0 \tag{32}$$

$$y_4 + y_5 - 1 = 0 \tag{33}$$

Second, the installation of either the multiphase transportation line or the combined installation of the oil and gas transportation lines is required

$$y_6 + y_8 - 1 = 0 \tag{34}$$

$$y_{11} + y_8 - 1 = 0 \tag{35}$$

Third, if multiphase boosting is chosen, then a multiphase pipeline is the only option

$$y_5 - y_8 \leq 0 \tag{36}$$

Fourth, the flow-line requires a corresponding riser to be installed (oil, gas or multiphase). And, if the phases are transported together, they must be separated by a topside separator.

Table A.1 Cost data for subsea flow-line and risers (Krogstad 2018)

	Size [In.]	Type	$C_{b,m}[10^6\ USD/km]$	$f_{s,m}[-]$	$C_{coat,m}[10^6\ USD/km]$	L_m
MP flowline (fm)	10	Rigid	0.230	1.00	0.360	d
MP riser (fr)	10	Flexible	2.300	1.70	0.360	w_d
Oil flowline (fo)	8	Rigid	0.230	0.72	0.290	d
Oil riser (ro)	8	Flexible	2.300	1.1	0.290	w_d
Gas flowline (fg)	4	Rigid	0.230	0.15	0.150	d
Gas riser (fr)	4	Flexible	2.300	0.5	0.150	w_d

$$y_8 = y_9 = y_{10} \tag{37}$$

$$y_6 = y_7 \tag{38}$$

$$y_{11} = y_{12} \tag{39}$$

The duties of the boosting and processing equipment vary over time, and they must be estimated in order to acquire the proper equipment size. The cooler area required is given by

$$A_c = x_{\text{c,max}} \frac{C_{\text{p,g}} \Delta T}{3.6 U_h \Delta T_{\text{LM}}}\ [\text{m}^2] \tag{40}$$

where $C_{\text{p,g}}$ is the heat capacity of the gas, ΔT is the temperature difference between the inflow and outflow of the gas, U_h is the heat transfer area, and ΔT_{LM} is the logarithmic mean temperature difference.

The processing equipment has a minimum intake pressure and it delivers a maximum pressure gain according to the equations below

$$p_{\text{in}} \geq 5000\ [\text{kPa}] \tag{41}$$

$$p_{\text{out}}(t) - p_{\text{in}} \leq 5000\ [\text{kPa}] \tag{42}$$

Regarding capacities, $x_{\text{c,max}}$, $x_{\text{p,max}}$, $x_{\text{ss,max}}$ and $x_{\text{ts,max}}$ represent the cooler, pump, subsea separator and topside separator maximum capacity, respectively:

$$x_{\text{c,max}} \geq x_{1,t}\ [\text{ton/h}] \tag{43}$$

$$x_{\text{p,max}} \geq x_{11,t}\ [\text{ton/h}] \tag{44}$$

$$x_{\text{ss,max}} \geq x_{2,t}\ [\text{ton/h}] \tag{45}$$

$$x_{\text{ts,max}} \geq x_{17,t}\ [\text{ton/h}] \tag{46}$$

The maximum power consumption of the compressor and pump are given by

$$P_{\text{k,max}} \geq P_k(t)\ [\text{kW}] \tag{47}$$

$$P_{\text{p,max}} \geq P_p(t)\ [\text{kW}] \tag{48}$$

The total initial investment is the sum of the costs of each installed equipment (in million dollars):

Table B.1 Composition employed in the simulation

Component $\text{GOR}_{\text{volume}} = 150\ Sm^3/Sm^3$	Mole fraction (mol/mol)
Nitrogen	3.70×10^{-03}
CO_2	1.10×10^{-03}
Methane	4.32×10^{-01}
Ethane	4.72×10^{-02}
Propane	2.97×10^{-02}
i-Butane	1.49×10^{-02}
n-Butane	9.30×10^{-03}
i-Pentane	8.30×10^{-03}
n-Pentane	5.00×10^{-03}
n-Hexane	1.83×10^{-02}
n-Heptane	4.11×10^{-02}
n-Octane	4.95×10^{-02}
n-Nonane	3.81×10^{-02}
22-Mpropane	2.00×10^{-04}
n-Decane	3.01×10^{-01}

Table C.1 Parameters used in the model

Symbol	Parameter	Value
α_0	Base operating time [h/year]	8000
β	Reservoir pressure decline coefficient [kPa]	6000
ΔT	Cooler temperature difference [K]	2.5
η_{mpp}	Multiphase pump efficiency [–]	0.60
η_{k}	Compressor efficiency [–]	0.75
η_{p}	Pump efficiency [–]	0.75
γ	Heat capacity ratio of the gas [–]	1.557
$\rho_{\text{g,std}}$	Gas density at standard conditions [ton/Sm^3]	0.000712
$\rho_{\text{o,std}}$	Oil density at standard conditions [ton/Sm^3]	0.844
a_1	Maximum production potential coefficient [–]	−43.40
a_2	Maximum production potential coefficient [–]	26.04
a_3	Maximum production potential coefficient [–]	−5.97
b_1	Maximum production potential coefficient [–]	0.38
b_2	Maximum production potential coefficient [–]	0.6
$C_{\text{p,g}}$	Gas heat capacity [J/(kg K)]	2681
d	Distance to coast [km]	8
f_I	Cost changes in time factor [–]	1.1035
f_{inst}	Installation cost factor [–]	4.208
f_{sub}	Subsea installation cost factor [–]	3
g	Gravitational acceleration [m/s^2]	9.81
GOR_{mass}	Gas-oil ratio in terms of mass [%wt]	0.06
M_{m}	Natural gas molar mass [kg/kmol]	16.804
O_{IIP}	Oil initially in place [ton]	85000000
$p_{r,0}$	Initial reservoir pressure [kPa]	9000
p_{ref}	Reference pressure [kPa]	20000
p_e	Electricity price [USD/kWh]	0.09
p_g	Gas price [USD/MMBtu]	2.61
p_o	Oil price [USD/bbl]	57.30
$q_{\text{ppo,0}}$	Maximum initial production potential when $p_s = 0$ [ton/h]	132
r	Interest rate [–]	10%
R	Universal gas constant [J/(mol K)]	8.314
T_{LM}	Cooler logarithmic mean temperature difference [K]	19.6
T_{i}	Gas temperature at the inlet of the compressor [K]	300
U_{h}	Heat transfer coefficient in the cooler [W/(m^2 K)]	20
U	Upper limit for mass flows [ton/h]	1000
w_{d}	Water depth [km]	0.2

$$C_0 = C_{\text{c}} + C_{\text{k}} + C_{\text{p}} + C_{\text{mpp}} + C_{\text{ss}} + C_{\text{ts}} + C_{\text{fg}} + C_{\text{rg}} + C_{\text{fm}} + C_{\text{rm}} + C_{\text{fo}} + C_{\text{ro}} \tag{49}$$

where C_{c} is the cooler cost, C_{k} is the compressor cost, C_{p} is the pump cost, C_{mpp} is the multiphase pump cost, C_{ss} is the subsea separator cost, C_{ts} is the topside separator cost, C_{fg} is the gas flow-line cost, C_{rg} is the gas riser cost, C_{fm} is the multiphase flow-line cost, C_{rm} is the multiphase riser cost, C_{fo} is the oil flow-line cost, and C_{ro} is the oil riser cost.

To estimate the cost of the installed equipment, cost correlations on the basic form

$$C_j = \left(a_j y_j + b_j S_j^n\right) f_1 f_2 \ldots \tag{50}$$

are used, where C_j is the estimated equipment cost for unit j, S_j is the size parameter, n is the cost exponent, a_j is the fixed cost, multiplied with the binary variable y_j for the corresponding piece of equipment. The b_j is a cost parameter dependent on the installed capacity. The f-factors are factors for additional cost adjustments. The cost equations used here are shown next.

The cost estimation for the cooler, compressor, pump, multiphase pump, subsea and topside separators are, respectively, given by

$$C_c = \left(0.024 \cdot y_1 + 0.000046 \cdot A_c^{1.2}\right) \cdot f_{\text{inst}} \cdot f_{\text{sub}} \cdot f_{\text{I}} \text{ [million USD]} \quad (51)$$

$$C_k = \left(0.49 \cdot y_3 + 0.0168 \cdot P_{\text{k,max}}^{0.6}\right) \cdot f_{\text{inst}} \cdot f_{\text{sub}} \cdot f_{\text{I}} \text{ [million USD]} \quad (52)$$

$$C_p = \left[0.00595 \cdot y_4 + 0.00177 \cdot P_{\text{p,max}}^{0.6} + 0.000206 \cdot \left(\frac{x_{\text{p,max}}}{3.6\rho_{\text{o,std}}}\right)^{0.9}\right] \cdot f_{\text{inst}} \cdot f_{\text{sub}} \cdot f_{\text{I}} \text{ [million USD]} \quad (53)$$

$$C_{\text{mpp}} = 3 \cdot f_{\text{inst}} \cdot f_{\text{I}} \cdot y_5 \text{ [million USD]} \quad (54)$$

$$C_{\text{ss}} = \left(0.414 \cdot y_2 + 0.054 \cdot x_{\text{ss,max}}\right) \cdot f_{\text{inst}} \cdot f_{\text{sub}} \cdot f_{\text{I}} \text{ [million USD]} \quad (55)$$

$$C_{\text{ts}} = 0.127 \cdot \left(x_{\text{ts,max}}\right)^{0.403} \quad (56)$$

where f_{inst}, f_{sub}, and f_{I} are cost factors for installation, subsea operation and cost changes in time, respectively.

The cost of the subsea flow-lines and risers are estimated from equation

$$C_m = \left(C_{\text{b,m}} \cdot f_{\text{s,m}} + C_{\text{coat,m}}\right) L_{\text{m}} \cdot y_{\text{m}} \text{ [million USD]} \quad (57)$$

where m is the type of riser or flowline, $C_{\text{b,m}}$ is the basic cost per unit length, $f_{\text{s,m}}$ is a cost size factor, $C_{\text{coat,m}}$ is the flow-line coating cost, and L_m is the length of the pipe: equals to d when from the wells to the FPSO, or equals to w_d from the seabed to the water surface. The cost is multiplied with the binary variable y_m corresponding to the installation of the unit. The data used for cost estimation of the flow-lines and risers is presented in Table A.1.

Appendix B. Fluid properties

The composition employed for the simulation is provided in Table B.1.

Appendix C. Input data

See table C.1

Acknowledgements This article has been written under the Norwegian Centre for Research-based Innovation on Subsea Production and Processing (SUBPRO). The authors greatly acknowledge the financial support by the Research Council of Norway, as well to the industrial partners involved in this project. We acknowledge the contributions by the late Dag Svenningsson Krogstad who developed the initial model as part of his master thesis.

Funding Open access funding provided by Norwegian University of Science and Technology. This study was funded by the Research Council of Norway and by industrial partners: Equinor and AkerBP, part of the SUBPRO project.

Declarations

Conflict of interest The authors declare that they have no known competing financial interests or personal relationships that could have appeared to influence the work reported in this paper.

References

Albuquerque FA, Vianna FLV, Alves RP, Kuchpil C, Morais MGG, Orlowski RTC, Moraes CAC, Ribeiro O (2013) Subsea processing systems: Future vision. In: Offshore Technology Conference. Offshore Technology Conference, Houston, USA, p. 14

Angga IGAG, Stanko M (2021) Automated decision support methodology for early planning phase of a multi-reservoir field. J Pet Sci Eng 205:108773

Bilal Pant M, Stanko M, Sales L (2021) Differential evolution for early-phase offshore oilfield design considering uncertainties in initial oil-in-place and well productivity. Upstream Oil Gas Technol 7:100055

Chidiac C, Holyfield S, Roberts I, Sauve R, Simpson N, Huynh U, Torres J (2019) Revolutionizing subsea field development planning through system integration and advanced diagnostics. In: Offshore Technology Conference. Offshore Technology Conference, p. 11

Devine MD, Lesso WG (1972) Models for the minimum cost development of offshore oil fields. Management Science. 18(8):B-378

Díaz Arias MJC, dos Santos AM, Altamiranda E (2021) Evolutionary Algorithm to Support Field Architecture Scenario Screening Automation and Optimization Using Decentralized Subsea Processing Modules. Processes 9(1):184

Fonseca dos Santos TD, Rocha DM, Pereira LI, Baioco JS, Albrecht CH, Jacob BP (2017) OTIMROTA-multiline: Computational tool for the conceptual design of subsea production systems. In: OTC Brasil. Offshore Technology Conference, Rio de Janeiro, Brazil, p. 13

GAMS Development Corporation (2021) General Algebraic Modeling System (GAMS). Fairfax, USA

Garcia-Diaz JC, Startzman R, Hogg GL (1996) A new methodology for minimizing investment in the development of offshore fields. SPE Prod Facil 11(01):22–29

González D, Stanko M, Hoffmann A (2020) Decision support method for early-phase design of offshore hydrocarbon fields using model-based optimization. J Pet Explor Prod Technol 10(4):1473–1495

Grimmett TT, Startzman RA (1987) Optimization of offshore field development to minimize investment. In: SPE Hydrocarbon Economics and Evaluation Symposium. Society of Petroleum Engineers, p. 11

Hong, C., Wang, Y., Yang, J., Berbert, Y. M., Lourenço, M. I., Estefen, S. F., Sep. 2017. Subsea production layout: design and cost. In: OMAE 2017. American Society of Mechanical Engineers Digital Collection, p. 7

John SM, Liu M-L, Wang Z, Lin J, (2018). Qualification of new technologies in subsea processing. In: Offshore Technology Conference. Offshore Technology Conference, Houston, USA, p. 12

Kocis G, Grossmann I (1989) Computational experience with dicopt solving minlp problems in process systems engineering. Comput Chem Eng 13(3):307–315

Krogstad DS (2018) Superstructure optimization of early stage offshore oil field development with subsea processing. MS thesis, Norwegian University of Science and Technology

Liberti L (2008) Introduction to global optimization. Ecole Polytechnique

Liu H, Gjersvik TB, Faanes A (2022) Subsea field layout optimization (part II)-the location-allocation problem of manifolds. J Pet Sci Eng 208:109273

Micali S, Abelsson C (2016) Novel subsea boosting solutions to increase IOR. In: Offshore Technology Conference Asia. OnePetro, Kuala Lumpur, Malaysia, p. 25

Mnasri H, Franchek MA, Wassar T, Tang Y, Meziou A (2022) Model-based simulation approach for pre-front end engineering design studies for subsea field architecture development. SPE Prod Oper 37(01):33–53

Moreno-Trejo J, Kumar R, Markeset T (2012) Mapping factors influencing the selection of subsea petroleum production systems: a case study. Int J Syst Assur Eng Manag 3(1):6–16

Offshore Magazine, (2020) Worldwide survey of subsea processing

Økland O, Davies SR, Rognø H (2013) Steps to the subsea factory. In: OTC Brasil. Offshore Technology Conference, Rio de Janeiro, Brazil, p. 10

Rodrigues HWL, Prata BA, Bonates TO (2016) Integrated optimization model for location and sizing of offshore platforms and location of oil wells. J Pet Sci Eng 145:734–741

Rosa VR, Ferreira Filho VJM (2013) Optimizing the location of platforms and manifolds. In: ASME 2012 31st International Conference on Ocean, Offshore and Arctic Engineering. American Society of Mechanical Engineers Digital Collection, pp. 813–818

Sahinidis NV (2021) BARON 21.1.13: Global Optimization of Mixed-Integer Nonlinear Programs, User's Manual

Sales L, Jäschke J, Stanko M (2021) Early field planning using optimisation and considering uncertainties - Study case: offshore deepwater field in Brazil. J Pet Sci Eng 207:109058

Sales LdPA, Pitombeira-Neto AR, Prata BdA (2018) A genetic algorithm integrated with Monte Carlo simulation for the field layout design problem. Oil Gas Sci Techno Revue d'IFP Energ nouvelles 73:16

Stape P, de Santana RSG, Baioco JS, Rocha DM, Jacob BP (2019) Influence of gathering system selection and positioning on flowline costs and production rates. In: The 29th International Ocean and Polar Engineering Conference. International Society of Offshore and Polar Engineers, pp. 2011–2017

Umeda T, Hirai A, Ichikawa A (1972) Synthesis of optimal processing system by an integrated approach. Chem Eng Sci 27(4):795–804